Chemistry of Diazaphospholephosphines. 2. Exocyclic Phosphine−Sulfido, −Selenido, and −Imido Derivatives of a Diazaphospholephosphine System. Crystal and Molecular Structures of Two Diazaphospholephosphine Imines: 4-(Difluoro((*p*-cyanotetrafluorophenyl)imino)phosphorano)-2,5-dimethyl-2*H*-1,2,3σ^2-diazaphosphole and 4-(Bis(dimethylamino)(((pentamethylcyclopentadienyl)dichlorotitanio)imino)phosphorano)-2,5-dimethyl-2*H*-1,2,3σ^2-diazaphosphole

Michael D. Mikoluk, Robert McDonald, and Ronald G. Cavell*

Department of Chemistry, University of Alberta, Edmonton, Alberta, Canada T6G 2G2

Received February 25, 1998

The substituted-exo-phosphine (X = F, NMe_2, OCH_2CF_3) diazaphospholephosphines are exclusively oxidized at this center with either chalcogens (S, Se) or azides to phosphoranodiazaphospholes. Oxidation imparts a dramatic upfield shift of the phosphorus NMR signals and an increase in the $^1J_{PC}$ coupling constants within the ring. (Difluorophosphino)diazaphosphole was also oxidized with selected amines using diethyl azodicarboxylate (DAD) as the coupling agent. Bulky amines (e.g., 2,4,6-tri-*tert*-butylaniline (mes*)) gave the monomeric iminophosphorane whereas less bulky amines (*p*-toluidine) formed mostly the cyclic diazadiphosphetidine. The crystal and molecular structure of 4-(difluoro((*p*-cyanotetrafluorophenyl)imino)phosphorano)-2,5-dimethyl-2*H*-1,2,3σ^2-diazaphosphole was determined: triclinic, $P\bar{1}$ (No. 2), a = 7.2744(15) Å, b = 10.087(4) Å, c = 10.566(2) Å, α = 66.62(2)°, β = 77.60(2)°, γ = 78.14(3)°, V = 688.8(4) Å^3, Z = 2. Final indices are R_1 = 0.0368 and wR_2 = 0.0968, and for all data, R_1 = 0.0478, wR_2 = 0.1033, and GOF = 1.067. The structure revealed two planar ring systems consisting of the diazaphosphole and the *p*-tetrafluorophenyl (tfbn) ring with an angle of 26.3° between the rings. The angle about the phosphine imine nitrogen (i.e., P═N−tfbn) is relatively open (141.2(2)°), and the P═N bond length is relatively short (1.514(2) Å). (((Trimethylsilyl)imino)(bis(dimethylamino))phosphorano)diazaphosphole gave, with Cp*$TiCl_3$, [(η^5-C_5Me_5)$TiCl_2$(N═P(NMe_2)$_2$(2,5-dimethyl-2*H*-1,2,3σ^2-diazaphosphol-4-yl))], which was also characterized structurally: monoclinic, $P2_1$ (No. 4), a = 11.9477(11) Å, b = 8.4757(6) Å, c = 12.7567(11) Å, β = 108.824(8)°, V = 1222.7(2) Å^3, Z = 2. Final indices are R_1 = 0.0630 and wR_2 = 0.1593, and for all data, R_1 = 0.0768, wR_2 = 0.1973, and GOF = 1.081. The Ti−N−P angle of 161.0(5)° was large, and the P═N distance (1.592(6) Å) and the Ti−N distance (1.781(6) Å) were both slightly shorter than those in similar titanium complexes. The P−N single bond distances between the exo-phosphorus atom and the attached dimethylamino groups were also short (1.649 Å (average)). These short values suggest delocalized bonding character throughout the metal−ligand framework, possibly a consequence of additional conjugation through the diazaphosphole ring.

Introduction

A major goal of our synthetic studies has been the controlled modification of diphosphorus compounds to induce differential reactivity in a potential ligand.[1−5] Oxidizing one phosphorus atom of a bis(phosphine) creates heterobifunctional phosphine ligand systems with contrasting (e.g., hard/soft) reactivities. Such systems provide coordinating ligands which offer both a phosphine and a heteroatom of different character (e.g., N, O, or S),[1−5] so that the coordination chemistry of the oxidized phosphorus center is then characterized by the newly introduced substituent. The previous phosphorus(III) center becomes part of the molecular backbone and contributes substitutional control and useful diagnostic ^{31}P NMR shift and coupling constant parameters. Oxidation with Me_3SiN_3 gives (trimethylsilyl)iminato derivatives which confer the further possibility of binding the metal via σ bonds through the elimination or migration of the trimethylsilyl group.[6−8] The imine nitrogen basicity is also easily varied by means of simple substitutions on this center[2,3] or through the use of other azides. Further control may be introduced through alteration of the backbone structure.[9] Oxidation of bis(phosphines) is however not easily controlled. Most reagents readily oxidize both phosphorus centers, a result which generally prevails with identically substituted phosphine centers. The diazaphospholephosphines provide a representative group of phosphine systems with both di- and tricoordinate P(III) centers,[10] the former in a ring

(1) Li, J.; Katti, K. V.; Pinkerton, A. A.; Nar, H.; Cavell, R. G. *Can. J. Chem.* **1996**, *74*, 2378−2385.
(2) Li, J.; Pinkerton, A. A.; Finnen, D. C.; Kummer, M.; Martin, A.; Wiesemann, F.; Cavell, R. G. *Inorg. Chem.* **1996**, *35*, 5684−5692.
(3) Li, J.; McDonald, R.; Cavell, R. G. *Organometallics* **1996**, *15*, 1033−1041.
(4) Balakrishna, M. S.; Santarsiero, B. D.; Cavell, R. G. *Inorg. Chem.* **1994**, *33*, 3079−3084.
(5) Balakrishna, M.; Klein, R.; Uhlenbrock, S.; Pinkerton, A. A.; Cavell, R. G. *Inorg. Chem.* **1993**, *32*, 5676−5681.
(6) Katti, K. V.; Cavell, R. G. *Organometallics* **1989**, *8*, 2147−2153.
(7) Katti, K. V.; Cavell, R. G. *Inorg. Chem.* **1989**, *28*, 3033−3036.
(8) Katti, K. V.; Cavell, R. G. *Inorg. Chem.* **1989**, *28*, 413−416.
(9) Reed, R. W.; Santarsiero, B.; Cavell, R. G. *Inorg. Chem.* **1996**, *35*, 4292−4300.

10.1021/ic9802101 CCC: $18.00
Published on Web 05/27/1999

Chart 1. Compound List and Ring-Numbering Scheme

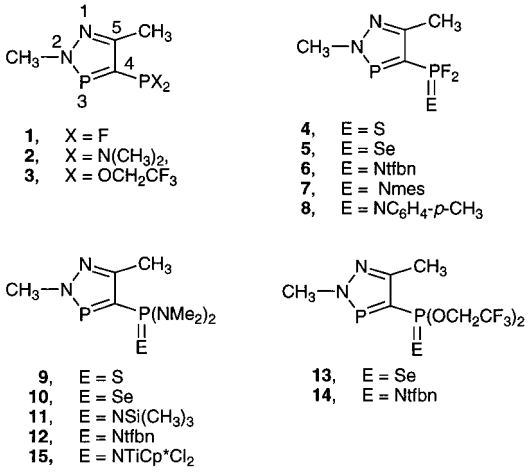

structure and the latter as an exocyclic phosphine which can be variously substituted with the usual procedures. Of interest were the different susceptibilities to oxidation for the two different phosphorus(III) centers and also the metal coordination chemistry of the system.

We previously described the synthesis of a selected series of mixed bis(phosphorus) compounds based on the diazaphospholylphosphine framework.[10] Herein we describe the chalcogen and imine oxidation of the exo-phosphine center in a series of diazaphospholylphosphines and also a transmetalation reaction with Ti. (All compounds are illustrated in Chart 1.) Further exploration of the complexation and binding behavior of these multifunctional diazaphospholephosphines will be presented in subsequent papers.[11,12]

Experimental Section

All experimental manipulations were performed under an atmosphere of dry argon using standard Schlenk techniques. Solvents were dried and freshly distilled prior to use; diethyl ether was distilled from sodium−benzophenone, hexane from sodium, and acetonitrile from P_2O_5, the last being stored over CaH_2. Deuterated solvents, $CDCl_3$ and CD_2Cl_2, were distilled over P_2O_5 and stored over molecular sieves under argon before use. Commercial reagents selenium, sulfur, diethyl azodicarboxylate (DEAD or DAD) (Aldrich), and trimethylsilyl azide (Lancaster) were used as received. All compounds used herein, the parent diazaphosphole, 4-(dichlorophosphino)-2,5-dimethyl-2*H*-1,2,3σ^2-diazaphosphole, and the derivatives thereof, 4-(difluorophosphino)-2,5-dimethyl-2*H*-1,2,3σ^2-diazaphosphole (**1**), (bis(dimethylamino)phosphino)-2,5-dimethyl-2*H*-1,2,3σ^2-diazaphosphole (**2**) and 4-(bis(2,2,2-trifluoroethoxy)phosphino)-2,5-dimethyl-2*H*-1,2,3σ^2-diazaphosphole (**3**), were prepared as described previously.[10]

NMR spectra were recorded on Bruker WH-200 and WH-400 spectrometers using the deuterium signal of the solvent as both the reference and the signal lock. The ^{1}H measurements were performed at 200.133 and 400.135 MHz, ^{13}C at 50.323 and 100.614 MHz, ^{31}P at 81.015 and 161.977 MHz, and ^{19}F at 188.313 and 376.503 MHz. External standards were $SiMe_4$ for ^{13}C and ^{1}H and 85% H_3PO_4 for ^{31}P. $CFCl_3$ was used as solvent, internal reference, and internal lock for ^{19}F NMR. Positive shifts lie downfield in all cases. NMR spectra were simulated with commercial packages.[13,14] Chemical ionization (CI) mass spectra were recorded using an AEI MS50 spectrometer exciting with ammonia at 16 eV. Low-resolution mass spectra (electron impact, EI) were recorded at 16 or 70 eV on an AEI MS50 spectrometer. Infrared spectra were recorded as CH_2Cl_2 casts on KBr cells using a Nicolet 7199 infrared spectrometer. Elemental analyses were performed by the Microanalytical Services Laboratory at the University of Alberta. Melting points were determined on samples in sealed melting point capillaries and are uncorrected.

Table 1. ^{31}P{^{1}H} NMR Data for Oxidized 4-Phosphorano-2,5-dimethyl-2*H*-1,2,3σ^2-diazaphospholes and the Parent Phosphines[a]

compd	X	E	$\delta(\sigma^2\text{P})$ (ppm)	$\delta(\sigma^4\text{P})$ (ppm)	$^2J_{\text{PP}}$ (Hz)
1	F	nothing[b]	255.03	208.84	107
4	F	S	264.25[c,e]	82.47[d,e]	112
5	F	Se	265.10[c]	87.50[d,f]	118
6	F	Ntfbn[g]	265.70[c]	2.66[d,h]	83
7	F	Nmes*[i]	266.38[c]	−40.56[d,j]	88
8	F	N(*p*-tol)[k]	266.41[c]	10.34[d,l]	96
2	$N(CH_3)_2$	nothing[b]	243.22	86.86	33
9	$N(CH_3)_2$	S	255.12[c]	70.83[c]	76
10	$N(CH_3)_2$	Se	257.19[c]	66.63[c,m]	84
11	$N(CH_3)_2$	$NSiMe_3$	253.50[c]	8.10[c]	68
12	$N(CH_3)_2$	Ntfbn[g]	257.29[c]	64.81[c]	65
3	OCH_2CF_3	nothing[b]	247.27	168.09	25
13	OCH_2CF_3	Se	259.01[c]	87.41[c,n]	108
14	OCH_2CF_3	Ntfbn[g]	260.12[c]	11.95[c]	84

[a] The structures are shown in Chart 1. Chemical shifts were referenced to 85% H_3PO_4, and measurements were performed in $CDCl_3$. [b] Reference 10. [c] Doublet. [d] Doublet of triplets. [e] Fluorine coupling: $^1J_{\text{PF}}$ 1133 Hz. [f] Fluorine coupling: $^1J_{\text{PF}}$ 1177 Hz. Selenium coupling: $^1J_{\text{PSe}}$ 1022 Hz. [g] tfbn = *p*-cyanotetrafluorophenyl. [h] Fluorine coupling: $^1J_{\text{PF}}$ 1145 Hz. [i] mes* = 2,4,6-tri-*tert*-butylbenzene. [j] Fluorine coupling: $^1J_{\text{PF}}$ 962 Hz. [k] *p*-tol = *p*-$CH_3C_6H_5$. [l] Fluorine coupling: $^1J_{\text{PF}}$ 971 Hz. [m] Selenium coupling: $^1J_{\text{PSe}}$ 751 Hz. [n] Selenium coupling: $^1J_{\text{PSe}}$ 893 Hz.

Table 2. Principal ^{13}C{^{1}H} NMR Data for Diazaphosphole Carbons in 4-Phosphino-2,5-dimethyl-2*H*-1,2,3σ^2-diazaphospholes[a,b]

compd	X	E	$^2J_{\sigma^2\text{PC}}$ (Hz)	$\delta(\text{C}^4)$ (ppm)	$^1J_{\sigma^2\text{PC}}$ (Hz)	$^1J_{\sigma^4\text{PC}}$ (Hz)	$\delta(\text{C}^5)$ (ppm)
4	F	S	17	141.21[d]	163	59	156.20[c]
5	F	Se	17	140.39[d]	160	64	155.46
6	F	Ntfbn[e]	18	125.17[d]	246	45	158.21[c]
7	F	Nmes*[f]	17	140.78[d]	159	61	155.78
8	F	N(*p*-tol)[g]	17	141.02[d]	165	60	156.12
9	$N(CH_3)_2$	S	18	144.68[d]	123	47	155.29[d]
10	$N(CH_3)_2$	Se	18	145.16[d]	157	43	154.54[c]
11	$N(CH_3)_2$	$NSiMe_3$	18	143.60[d]	155	49	156.27[d]
12	$N(CH_3)_2$	Ntfbn[e]	18	134.03[d]	147	52	156.78[d]
13	OCH_2CF_3	Se	18	142.17	144	43	155.66
14	OCH_2CF_3	Ntfbn[e]	18	128.79	139	53	156.31[d]

[a] The structures are shown in Chart 1. Chemical shifts were referenced to $SiMe_4$. [b] In $CDCl_3$. [c] Doublet. [d] Doublet of doublets. [e] tfbn = *p*-cyanotetrafluorophenyl. [f] mes* = 2,4,6-tri-*tert*-butylbenzene. [g] *p*-tol = *p*-$CH_3C_6H_5$.

Sulfur and Selenium Oxidation of the Phosphinodiazaphospholes. (a) 4-(Difluorothioxophosphorano)-2,5-dimethyl-2*H*-1,2,3σ^2-diazaphosphole (4). Sulfur (0.116 g, 3.6 mmol) was added to a solution of **1** (0.5 mL, 3.6 mmol) in 10 mL of toluene, and the mixture was heated to reflux for 48 h. The solvent was removed in vacuo, to leave a yellow liquid which contained some sulfur. Diethyl ether was added (5 mL), and the solution was filtered through Celite. The ether and excess **1** were then removed in vacuo, to leave **4** as a light yellow oil. Yield: 0.403 g (52.3%). Anal. Calcd for $C_4H_6F_2N_2P_2S$: C, 22.44; H, 2.82; N, 13.08; S, 14.97. Found: C, 22.42; H, 2.95; N, 13.09; S, 14.79. MS (EI, *m*/*z*): 214 (M, 29%), 182 (M − S, 100%). IR (CH_2Cl_2 cast, cm^{-1}): ν(P═S) 726 (w), ν(P−F) 853 (s), 823 (s). NMR ($CDCl_3$): see Tables 1−3. Other NMR parameters are as follows. ^{13}C{^{1}H}: C−CH_3 δ 14.75 (s), P(σ^2)−N−CH_3 δ 41.49 (d, $^2J_{\sigma^2\text{PC}}$ 17 Hz), P−C^4−P ($^2J_{\text{CF}}$ 24.1 Hz),

(10) Part 1 of this series: Cavell, R. G.; Mikoluk, M. D. *Inorg. Chem.* **1999**, *38*, 1971−1981.
(11) Part 3 of this series: Cavell, R. G.; Mikoluk, M. D. *Organometallics*, in press.
(12) Part 4 of this series: Cavell, R. G.; Mikoluk, M. D. *Inorg. Chem.*, in press.
(13) *Parameter Adjustment in NMR by Iteration Calculation (PANIC)*; Bruker Instrument Co.: Karlsrühe, Germany.
(14) Spectra simulated with gNMR: Budzelaar, G. M. *gNMR (4.0)*; Cherwell Scientific Publishing Co.: Oxford, U.K., 1997.

Table 3. Principal ^{1}H NMR Data for Diazphosphole Protons in Oxidized 4-Phosphorano-2,5-dimethyl-2*H*-1,2,3σ^2-diazaphospholes[a]

compd	X	E	δ(CH$_3$−N) (ppm)	$^3J_{\sigma^2\mathrm{PH}}$ (Hz)	δ(C−CH$_3$) (ppm)
4	F	S	3.94[b]	8.6	2.39[b]
5	F	Se	4.02[b]	8.6	2.51[c]
6	F	Ntfbn[d]	4.14[b]	8.9	2.61[c]
7	F	Nmes* [e]	4.03[b]	8.4	2.59[c]
8	F	N(*p*-tol)[f]	4.03[b]	8.3	2.59[c]
9	N(CH$_3$)$_2$	S	3.95[b]	7.7	2.51[g]
10	N(CH$_3$)$_2$	Se	3.95[b]	7.9	2.64[g]
11	N(CH$_3$)$_2$	NSiMe$_3$	3.88[b]	7.4	2.41[b]
12	N(CH$_3$)$_2$	Ntfbn[d]	3.97[b]	7.9	2.42[b]
13	OCH$_2$CF$_3$	Se	3.96[b]	8.4	2.48[c]
14	OCH$_2$CF$_3$	Ntfbn[d]	4.01[b]	8.6	2.51[c]

[a] The structures are shown in Chart 1. Chemical shifts were referenced to SiMe$_4$ measured in CDCl$_3$. [b] Doublet. [c] Singlet. [d] tfbn = *p*-cyanotetrafluorophenyl. [e] mes* = 2,4,6-tri-*tert*-butylbenzene. [f] *p*-tol = *p*-CH$_3$C$_6$H$_5$. [g] Doublet of doublets.

Table 4. ^{77}Se NMR Data for 4-(Selenoxophosphorano)-2,5-dimethyl-2*H*-1,2,3σ^2-diazaphospholes[a]

compd	δ(Se) (ppm)	$^1J_{\sigma^4\mathrm{PSe}}$ (Hz)	$^3J_{\sigma^2\mathrm{PSe}}$ (Hz)
5		1022	
10	−245.04[b]	751	41
14	−249.61[b]	893	30

[a] The structures are shown in Chart 1. Chemical shifts were referenced to Me_2Se_2 and measured in $CDCl_3$. [b] Doublet.

N−*C*^{5}−CH$_3$ δ 156.29 (d, $^2J_{\sigma^4\mathrm{PC}}$ 1 Hz). ^{19}F: δ −41.84 (dd, $^1J_{\sigma^4\mathrm{PF}}$ 1132 Hz, $^3J_{\sigma^4\mathrm{PF}}$ 6 Hz).

(b) 4-(Difluoroselenoxophosphorano)-2,5-dimethyl-2*H*-1,2,3σ^2-diazaphosphole (5). Selenium (0.592 g, 7.5 mmol) was added to a solution of **1** (1.00 mL, 7.2 mmol) in 15 mL of toluene, and the mixture was heated to reflux for 12 h. The solution was cooled and then filtered through Celite. The precipitate was washed with (2 × 5 mL) toluene, and the solvent was removed in vacuo, to leave **5** as colorless moisture-sensitive crystals. Yield: 1.80 g (95.6%). Anal. Calcd for $C_4H_6F_2N_2P_2Se$: C, 18.41; H, 2.32; N, 10.73. Found: C, 18.02; H, 2.16; N, 10.58. MS (EI, *m*/*z*): 262 (M, 26%), 182 (M − Se, 100%). IR (CH_2Cl_2 cast, cm^{-1}): ν(P═Se) 533 (m), ν(P−F) 869 (s), 841 (s). NMR ($CDCl_3$): see Tables 1−4. Other NMR parameters are as follows. ^{1}H: C−C*H*$_3$ δ 2.51 (s), P(σ^2)−N−C*H*$_3$ δ 4.02 (d, $^3J_{\sigma^2\mathrm{PH}}$ 8.6 Hz). ^{13}C{^{1}H}: C−*C*H$_3$ δ 15.10 (s), P(σ^2)−N−*C*H$_3$ δ 41.79 (d, $^2J_{\sigma^2\mathrm{PC}}$ 17 Hz). ^{19}F: δ −43.03 (dd, $^1J_{\sigma^4\mathrm{PF}}$ 1169 Hz, $^3J_{\sigma^2\mathrm{PF}}$ 34 Hz).

(c) 4-(Bis(dimethylamino)thioxophosphorano)-2,5-dimethyl-2*H*-1,2,3σ^2- diazaphosphole (9). Sulfur (0.154 g, 4.8 mmol) was added to a solution of **2** (1.0 mL, 4.8 mmol) in 10 mL of toluene, and the mixture was heated to reflux for 48 h. The solvent was removed in vacuo, to leave impure **9** as a yellow liquid which contained some sulfur. Diethyl ether was added (5 mL), and the solution was filtered through Celite. The ether was then removed in vacuo, to give pure **9**. Yield: 1.14 g (89.5%). Mp = 135−138 °C. Anal. Calcd for $C_8H_{18}N_4P_2S$: C, 36.36; H, 6.87; N, 21.20; S, 12.13. Found: C, 36.42; H, 6.95; N, 21.09; S, 11.79. MS (EI, *m*/*z*): 264 (M, 80%). IR (CH_2Cl_2 cast, cm^{-1}): ν(P═S) 723 (w), ν(P−N) 735 (s), 715 (s). NMR ($CDCl_3$): see Tables 1−4. Other NMR parameters are as follows. ^{1}H: C−C*H*$_3$ δ 2.51 (dd, $^4J_{\mathrm{PH}}$ 1.5 Hz, $^4J_{\sigma^2\mathrm{PH}}$ 0.5 Hz), P(σ^2)−N−C*H*$_3$ δ 3.95 (d, $^3J_{\sigma^2\mathrm{PH}}$ 7.7 Hz). ^{13}C{^{1}H}: C−*C*H$_3$ δ 15.60 (s), P(σ^2)−N−*C*H$_3$ δ 41.18 (d, $^2J_{\sigma^2\mathrm{PC}}$ 18 Hz), N−*C*^{5}−CH$_3$ δ 155.29 (dd, $^2J_{\sigma^2\mathrm{PC}}$ 5 Hz, $^2J_{\sigma^4\mathrm{PC}}$ 5 Hz), P(σ^4)−N−*C*H$_3$ δ 40.29 (d, $^2J_{\sigma^4\mathrm{PC}}$ 5 Hz).

(d) 4-(Bis(dimethylamino)selenoxophosphorano)-2,5-dimethyl-2*H*-1,2,3σ^2-diazaphosphole (10). Selenium (0.381 g, 4.8 mmol) was added to a solution of **2** (1.0 mL, 4.8 mmol) in 10 mL of toluene, and the mixture was heated to reflux for 12 h. The solution was cooled and then filtered through Celite. The precipitate was washed with (2 × 5 mL) toluene, and the solvent was removed in vacuo, to leave **10** as off-white, moisture-sensitive crystals, which were recrystallized from toluene. Yield: 1.47 g (96.7%). Anal. Calcd for $C_8H_{18}N_4P_2Se$: C, 30.88; H, 5.83; N, 18.01. Found: C, 31.02; H, 5.90; N, 17.78. Mp = 148−150 °C. IR (CH_2Cl_2 cast, cm^{-1}): ν(P═Se) 542 (m), ν(P−N) 716 (s), 692 (s). MS (CI, *m*/*z*): 313 (M + 1, 100%). NMR ($CDCl_3$): see Tables 1−4. Other NMR parameters are as follows. ^{1}H: C−C*H*$_3$ δ 2.64 (dd, $^4J_{\mathrm{PH}}$ 1.1 Hz, $^4J_{\mathrm{PH}}$ 1.1 Hz), P(σ^2)−N−C*H*$_3$ δ 3.95 (d, $^3J_{\sigma^2\mathrm{PH}}$ 7.9 Hz). ^{13}C{^{1}H}: C−*C*H$_3$ δ 15.84 (s), P(σ^2)−N−*C*H$_3$ δ 41.21 (d, $^2J_{\sigma^2\mathrm{PC}}$ 18 Hz), N−*C*^{5}−CH$_3$ δ 155.27 (d, $^2J_{\sigma^4\mathrm{PC}}$ 5 Hz), P(σ^4)−N−*C*H$_3$ δ 40.54 (d, $^2J_{\sigma^4\mathrm{PC}}$ 5 Hz).

(e) 4-(Bis(2,2,2-trifluoroethoxy)selenoxophosphorano)-2,5-dimethyl-2*H*-1,2,3σ^2-diazaphosphole (13). Selenium (0.205 g, 2.6 mmol) was added to a solution of **3** (0.135 g, 2.5 mmol) in 10 mL of toluene, and the mixture was heated to reflux for 12 h. The solution was cooled and then filtered through Celite. The precipitate was washed with (2 × 5 mL) toluene, and the solvent was removed in vacuo, to leave **13** as off-white, moisture-sensitive crystals, which were recrystallized from toluene. Yield: 1.03 g (98.2%). Anal. Calcd for $C_8H_{10}F_6N_2O_2P_2Se$: C, 22.82; H, 2.39; N, 6.65. Found: C, 22.51; H, 2.45; N, 6.62. Mp = 132−134 °C. MS (EI, *m*/*z*): 422 (M, 100%). IR (CH_2Cl_2 cast, cm^{-1}): ν(P═Se) 542 (m). NMR ($CDCl_3$): see Tables 1−3. Other NMR parameters are as follows. ^{1}H: C−C*H*$_3$ δ 2.48 (s), P(σ^4)−N−O−C*H*$_2$-CF$_3$ δ 2.39 (m). ^{13}C{^{1}H}: C−*C*H$_3$ δ 14.77 (s), P(σ^2)−N−*C*H$_3$ δ 41.38 (d, $^2J_{\mathrm{PC}}$ 18 Hz), N−*C*^{5}−CH$_3$ δ 155.66 (br s), P(σ^4)−O−*C*H$_2$−CF$_3$ δ 65.68 (dq, $^2J_{\sigma^4\mathrm{PC}}$ 6 Hz, $^2J_{\mathrm{FC}}$ 36 Hz), P(σ^4)−O−CH$_2$−*C*F$_3$ δ 123.89 (dq, $^3J_{\sigma^4\mathrm{PC}}$ 6 Hz, $^1J_{\mathrm{FC}}$ 278 Hz). ^{19}F: δ −75.20 (t, $^3J_{\mathrm{FH}}$ 8 Hz). ^{77}Se: δ −249.61 (dd, $^3J_{\sigma^2\mathrm{PF}}$ 30 Hz, $^1J_{\sigma^3\mathrm{PF}}$ 893 Hz).

Synthesis of Iminophosphorane Derivatives. (i) Azide Oxidation. (a) 4-(Difluoro((*p*-cyanotetrafluorophenyl)imino)phosphorano)-2,5-dimethyl-2*H*-1,2,3σ^2-diazaphosphole (6). *p*-Cyanotetrafluorophenyl azide (1.0 mL, 7.2 mmol) was added dropwise with a syringe to a stirred solution containing **1** (1.0 mL, 7.2 mmol) dissolved in 15 mL of dichloromethane at −78 °C (acetone/dry ice). The solution, which became yellow a few minutes after the addition, was left to warm to room temperature (22 °C) with continuous stirring overnight. At the end of the reaction period, the solution was colorless. The volume of the solution was reduced to ∼5 mL, and the solution was stored at −40 °C overnight, to produce colorless crystals of **6**. Yield: 2.39 g (89.7%). Mp = 123 °C. Anal. Calcd for $C_{11}H_6F_6N_4P_2$: C, 35.70; H, 1.63; N, 15.14. Found: C, 35.12; H, 1.68; N, 15.28. MS (EI, *m*/*z*): 370 (M, 100%). IR (CH_2Cl_2 cast, cm^{-1}): ν(P═N) 1498 (s), ν(P−F) 921 (s), 896 (s), ν(CN) 2241 (s). NMR ($CDCl_3$): see Tables 1−3. Other NMR parameters are as follows. ^{13}C{^{1}H}: C−*C*H$_3$ δ 15.01 (s), P(σ^2)−N−*C*H$_3$ δ 41.92 (d, $^2J_{\sigma^2\mathrm{PC}}$ 18 Hz), N−*C*^{5}−CH$_3$ δ 158.21 (d, $^2J_{\sigma^4\mathrm{PC}}$ 13 Hz). ^{19}F: δ −56.54 (dd, $^1J_{\mathrm{PF}}$ 1169 Hz, $^3J_{\mathrm{PF}}$ 34 Hz), *m*-F of tfbn δ 139.77 (m), *o*-F of tfbn δ −152.81 (m).

(b) 4-(Bis(dimethylamino)((trimethylsilyl)imino)phosphorano)-2,5-dimethyl-2*H*-1,2,3σ^2-diazaphosphole (11). Trimethylsilyl azide (1.3 mL, 10 mmol) was added to a solution of **2** (0.5 mL, 4.8 mmol) in 10 mL of acetonitrile, and the mixture was heated to reflux for 24 h. The solution was then cooled, and the volatile materials were removed in a vacuum, to leave **11** as a light amber oil. MS (EI, *m*/*z*): 319 (M, 37%). IR (CH_2Cl_2 cast, cm^{-1}): ν(P═N) 1492 (s), ν(P−N) 851 (s), 816 (s). NMR ($CDCl_3$): see Tables 1−3. Other NMR parameters are as follows. ^{1}H: Si−C*H*$_3$ δ 0.12 (s). ^{13}C{^{1}H}: C−*C*H$_3$ δ 15.05 (s), P(σ^2)−N−*C*H$_3$ δ 40.75 (d, $^2J_{\sigma^2\mathrm{PC}}$ 18 Hz), N−*C*^{5}−CH$_3$ δ 156.72 (dd, $^2J_{\sigma^2\mathrm{PC}}$ 7 Hz, $^2J_{\sigma^4\mathrm{PC}}$ 7 Hz), P(σ^4)−N−*C*H$_3$ δ 40.27 (d, $^2J_{\sigma^4\mathrm{PC}}$ 7 Hz).

(c) 4-(Bis(dimethylamino)((*p*-cyanotetrafluorophenyl)imino)-phosphorano)-2,5-dimethyl-2*H*-1,2,3σ^2-diazaphosphole (12). *p*-Cyanotetrafluorophenyl azide (0.7 mL, 4.8 mmol) was added dropwise with a syringe to a stirred solution containing **2** (0.5 mL, 4.8 mmol) dissolved in 15 mL of dichloromethane at −78 °C (acetone/dry ice). The solution adopted a yellow color a few minutes after the addition. The solution was then allowed to warm to room temperature (22 °C) slowly, and stirring was continued overnight; by this time, the solution was colorless. The solvent was removed in a vacuum, to leave **12** as off-white, moisture-sensitive crystals. Yield: 1.51 g (75.3%). Anal. Calcd for $C_{15}H_{18}F_4N_6P_2$: C, 42.87; H, 4.32; N, 20.00. Found: C, 42.67; H, 4.25; N, 20.09. Mp = 152 °C dec. MS (EI, *m*/*z*): 420 (M, 100%). IR (CH_2Cl_2 cast, cm^{-1}): ν(P═N) 1377 (s), ν(P−N) 862 (s), 828 (s), ν(CN) 2237 (s). NMR ($CDCl_3$): see Tables 1−3. Other NMR parameters are as follows. ^{13}C{^{1}H}: C−*C*H$_3$ δ 15.95 (s), P(σ^2)−N−

CH_3 δ 41.24 (d, $^2J_{\sigma^2PC}$ 18 Hz), N−C^5−CH_3 δ 156.78 (dd, $^2J_{\sigma^2PC}$ 5 Hz, $^2J_{\sigma^4PC}$ 5 Hz), P(σ^4)−N−CH_3 δ 40.78 (d, $^2J_{\sigma^4PC}$ 5 Hz). ^{19}F (second order): *m*-F of tfbn δ 139.77, *o*-F of tfbn δ −152.81.

(d) 4-(Bis(2,2,2-trifluoroethoxy)((*p*-cyanotetrafluorophenyl)imino)phosphorano)-2,5-dimethyl-2*H*-1,2,3σ^2-diazaphosphole (14). *p*-Cyanotetrafluorophenyl azide (0.4 mL, 2.5 mmol) was added dropwise by means of a syringe to a stirred solution containing **3** (0.141 mL, 2.5 mmol) dissolved in 15 mL of dichloromethane. The solution was maintained at −78 °C (acetone/dry ice). The solution, which became yellow a few minutes after the addition, was then left to warm to room temperature (22 °C) with continuous stirring overnight; by this time, the solution was colorless. The solvent was removed in a vacuum, to leave **14** as off-white crystals, which were recrystallized from toluene. Yield: 1.09 g (82.3%). Anal. Calcd for $C_{15}H_{10}F_{10}N_4O_2P_2$: C, 33.98; H, 1.90; N, 10.57. Found: C, 33.62; H, 1.79; N, 10.55. Mp = 122 °C. MS (EI, *m*/*z*): 530 (M, 31%). IR (CH_2Cl_2 cast, cm^{-1}): ν(P=N) 1489 (s), ν(CN) 2235 (m). NMR ($CDCl_3$): see Tables 1−3. Other NMR parameters are as follows. ^{13}C{^{1}H}: C−CH_3 δ 14.98 (s), P(σ^2)−N−CH_3 δ 41.45 (d, $^2J_{\sigma^2PC}$ 18 Hz), P−C^4−P δ 128.79 (dd, $^2J_{\sigma^2PC}$ 139 Hz, $^2J_{\sigma^4PC}$ 53 Hz), N−C^5−CH_3 δ 156.31 (dd, $^2J_{\sigma^2PC}$ 5 Hz, $^2J_{\sigma^4PC}$ 5 Hz), P(σ^4)−O−CH_2−CF_3 δ 66.08 (dq, $^2J_{\sigma^4PC}$ 5 Hz, $^2J_{FC}$ 36 Hz), P(σ^4)−O−CH_2−CF_3 δ 124.21 (q, $^1J_{FC}$ 278 Hz). ^{19}F: δ −75.43 (t, $^3J_{FH}$ 8 Hz), *m*-F of tfbn δ 139.77, *o*-F of tfbn δ −152.81.

(ii) Redox Condensation. (a) 4-(Difluoro((2,4,6-tri-*tert*-butylphenyl)imino)phosphorano)-2,5-dimethyl-2*H*-1,2,3σ^2-diazaphosphole (7). A solution of diethyl 1,2-hydrazinedicarboxylate (0.6 mL, 3.8 mmol) in 5 mL of THF was added dropwise over a 30 min period to a stirred solution containing **1** (0.5 mL, 3.6 mmol) and 2,4,6-tri-*tert*-butylaniline (0.941 g, 3.6 mmol) dissolved in 10 mL of THF which was maintained at 0 °C. The solution was then stirred for 12 h at room temperature (22 °C). The initial red color of the solution which formed on mixing the reagents slowly disappeared within a few hours after the addition was begun. The pure product could not be isolated. Some spectroscopic characterization data were obtained for **7**. MS (EI, *m*/*z*): 441 (M, 15%). NMR ($CDCl_3$): see Tables 1−3. Other NMR parameters are as follows. ^{1}H: N−C−CH_3 δ 2.59 (s), P(σ^2)−N−CH_3 δ 4.03 (d, $^3J_{\sigma^2PH}$ 8.4 Hz), ^{t}Bu CH_3 δ 1.39 (s). ^{13}C{^{1}H}: C−CH_3 δ 15.02 (s), P(σ^2)−N−CH_3 δ 41.81 (d, $^1J_{\sigma^2PC}$ 17 Hz), N−C^5−CH_3 δ 155.78 (s). ^{19}F: δ −58.41 (dd, $^1J_{\sigma^2PF}$ 1079 Hz, $^3J_{\sigma^3PF}$ 10 Hz).

(b) 4-(Difluoro((*p*-methylphenyl)imino)phosphorano)-2,5-dimethyl-2*H*-1,2,3σ^2-diazaphosphole (8). A solution of diethyl 1,2-hydrazinedicarboxylate (0.6 mL, 3.9 mmol) in 5 mL of THF was slowly added dropwise (over 30 min) to a stirred solution containing **1** (0.5 mL, 3.6 mmol) and *p*-toluidine (0.386 g, 3.6 mmol) dissolved in 10 mL of THF at 0 °C. The solution was then stirred at room temperature (22 °C) for 12 h. The initial red color of the solution slowly lightened over a period of a few hours following the completion of the addition. The pure product could not be isolated. Some spectroscopic characterization data were obtained for **8**. MS (EI, *m*/*z*): 287 (M, 100%). NMR ($CDCl_3$): see Tables 1−3. Other NMR parameters are as follows. ^{13}C{^{1}H}: C−CH_3 δ 14.97 (s), P(σ^2)−N−CH_3 δ 41.83 (d, $^2J_{\sigma^2PC}$ 17 Hz). ^{19}F: δ −58.41 (d (broad), $^1J_{PF}$ 971 Hz).

Transmetalation Reaction: Synthesis of [(η^5-C_5Me_5)$TiCl_2$(N=P-(NMe_2)$_2$(2,5-dimethyl-2*H*-1,2,3σ^2-diazaphosphol-4-yl))] (15). Trimethylsilyl azide (0.65 mL, 5 mmol) was added to a solution of **3** (0.25 mL, 2.4 mmol) in 10 mL of acetonitrile, and the mixture was heated to reflux for 24 h, to give **11** in solution. The solution was cooled, and the volatiles were removed in vacuo. Fresh acetonitrile (15 mL) was then added to this flask along with Cp*$TiCl_3$ (0.695 g, 4.8 mmol). The solution was refluxed for a period of 24 h. As the solution cooled to room temperature, orange crystals appeared. The yield of **15** was 9.84 g (62.8%). Mp = 145 °C dec. Anal. Calcd for $C_{18}H_{33}Cl_2N_5P_2Ti$: C, 43.22; H, 6.65; Cl, 14.12; N, 14.00. Found: C, 43.32; H, 6.72; Cl, 14.26; N, 14.08. MS (FAB, *m*/*z*): 500 (M + 1, 5%). IR (CH_2Cl_2 cast, cm^{-1}): ν(P−N−Ti) 1091 (s). NMR data ($CDCl_3$) are as follows. ^{31}P-{^{1}H}: P(σ^2) δ 260.87 (d, $^2J_{PP}$ 84 Hz), P(σ^3) δ 40.87 (d, $^2J_{PP}$ 84 Hz). ^{1}H: C−CH_3 δ 2.43 (dd, $^4J_{PH}$ 0.9 Hz), P(σ^2)−N−CH_3 δ 4.03 (d, $^3J_{PH}$ 12.2 Hz), P(σ^3)−N−CH_3 δ 3.76 (d, $^3J_{PH}$ 8.2 Hz), C^5−(CH_3)$_5$ δ 1.98 (s). ^{13}C{^{1}H}: C−CH_3 δ 14.37 (s), P(σ^2)−N−CH_3 δ 41.88 (d, $^2J_{PC}$ 18 Hz), P(σ^3)−N−CH_3 δ 40.03 (d, $^2J_{PC}$ 3 Hz), P−C−P δ 143.25 (dd, $^2J_{\sigma^2PC}$ 45 Hz, $^2J_{\sigma^3PC}$ 23 Hz), N−C−CH_3 δ 156.72 (dd, $^2J_{\sigma^2PC}$ 5 Hz, $^2J_{\sigma^3PC}$ 18 Hz), C^5−(CH_3)$_5$ δ 97.78 (s), C^5−(CH_3)$_5$ δ 9.93 (s).

Results and Discussion

Synthetic Considerations.

A. Oxidation of 4-(Disubstituted phosphino)-2,5-dimethyl-2*H*-1,2,3σ^2-diazaphospholes (1−3) with Chalcogens. The chalcogen (sulfur or selenium) oxidation of the phosphorus(III) center in **1**, **2**, or **3** proceeded smoothly in a direct reaction of the elemental chalcogen with the phosphine under controlled conditions (eq 1). Examination of the reaction mixtures before

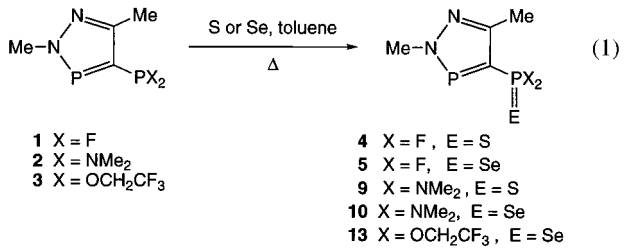

(1)

1 X = F
2 X = NMe_2
3 X = OCH_2CF_3

4 X = F, E = S
5 X = F, E = Se
9 X = NMe_2, E = S
10 X = NMe_2, E = Se
13 X = OCH_2CF_3, E = Se

separation revealed that stoichiometric control of the reactant ratio yielded only the monosulfide or monoselenide. Any unreacted chalcogen was removed by Celite filtration in the purification procedure. We note also that the NMR-active ^{77}Se nucleus readily identifies the oxidized phosphorus in these cases. In contrast to the reaction with sulfur, the selenium reaction proceeded more quickly to give a higher yield (crystallized 87%) of **5** after a 12 h reaction. The analogous preparation of **4** required a much longer reaction time, and the isolated yield was lower (43%). Both compounds were extremely sensitive toward moisture.

This difluoro sulfide was previously identified by NMR in an unseparated mixture with the chloro fluoro sulfide obtained upon reaction of 4-(dichlorothioxophosphorano)diazaphosphole with zinc fluoride (eq 2).[15]

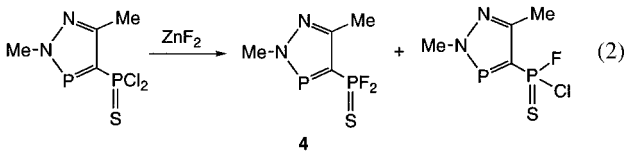

(2)

4

In a similar fashion, oxidation of **2** with sulfur and selenium in refluxing toluene (eq 1) gave the white crystalline products **9** (E = S) and **10** (E = Se), respectively, and **3** reacted with Se (1 day, refluxing toluene) to give **13**. Compounds **9**, **10**, and **13** were less sensitive toward moisture than **4** and **5**.

B. Imine Formation. (i) Via Azide Oxidation. General routes from phosphines to phosphine imines are provided by either (a) the Staudinger reaction[8,16] with azides or (b) the redox condensation reaction with an amine in the presence of diethyl azodicarboxylate (abbreviated DEAD or DAD).[17] Staudinger imination of 4-(difluorophosphino)-2,5-dimethyl-2*H*-1,2,3σ^2-phosphole (**1**) with *p*-cyanotetrafluorophenyl azide at −78 °C in dichloromethane proceeded smoothly to yield the heterobifunctional phosphoranophosphine **6** (eq 3), in which the exo-phosphorus center was exclusively oxidized. Recrystalli-

(15) Weinmaier, J. H.; Brunnhuber, G.; Schmidpeter, A. *Chem. Ber.* **1980**, *113*, 2278−2290.
(16) Staudinger, H.; Meyer, J. *Helv. Chim. Acta* **1919**, *2*, 635−646.
(17) Bittner, S.; Assaf, Y.; Krief, P.; Pomerantz, M.; Ziemnicka, B. T.; Smith, C. G. *J. Org. Chem.* **1985**, *50*, 1712−1718.

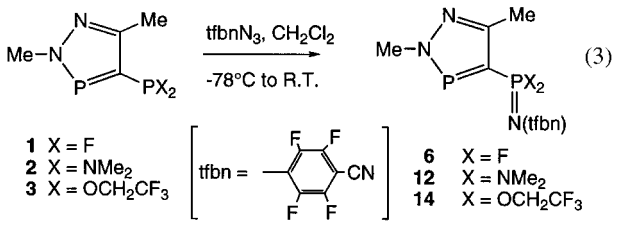

zation from dichloromethane at −40 °C gave colorless crystals of X-ray quality. The structural characterization of **6** is described below.

Similarly, the (aminophosphino)phosphole **2** reacted rapidly with *p*-cyanotetrafluorophenyl azide (in dichloromethane solution at −78 °C, eq 3) to give **12**, and again, only the exocyclic aminophosphine center was oxidized. This (aminophosphino)-phosphole, **2**, could also be treated with trimethylsilyl azide, which reacted cleanly with **2** under refluxing conditions in toluene (eq 4) to give **11**; only the exocyclic phosphorus was

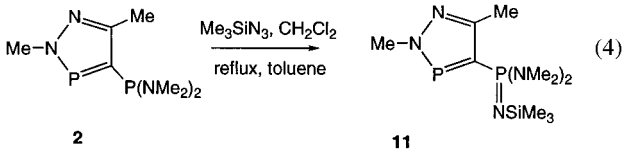

oxidized, and use of excess trimethylsilyl azide did not yield further oxidation. The trimethylsilyl azide reaction with **1** was not clean.

In a similar fashion, **3** reacted with *p*-cyanotetrafluorophenyl azide (eq 3) to give **14** as a white solid in 84% yield. Color changes observed in the course of all reactions suggested the formation of phosphazide intermediates.[18,19] The eventual products were light amber oils.

(ii) Via Redox Condensation of (Fluorophosphino)diazaphospholes with Diethyl Azodicarboxylate. The redox condensation reaction of a primary amine with a phosphine with removal of the protons by diethyl azodicarboxylate (DAD) provides an alternate route to variously substituted imine derivatives which is potentially attractive because the procedure avoids dangerous azides. The reaction of 4-(bis(dimethylamino)-phosphino)-2,5-dimethyl-2*H*-1,2,3σ^2-diazaphosphole with either 2,4,6-tri-*tert*-butylaniline (mes*NH_2) or *p*-toluidine in the presence of DAD gave the σ^2P−σ^4P (iminophosphorano)diazaphosphole **7** or **8** (eq 5), respectively, as the major product in the

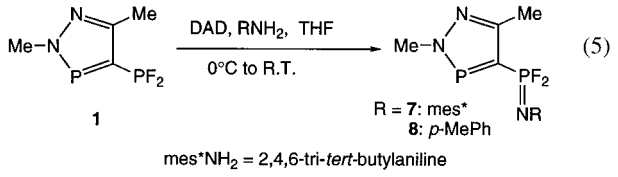

former case and as a minor product in the latter. The other product of this reaction was the dimeric phosphetidine (vide infra).

The reaction proceeds via the betaine intermediate **1-B** (Scheme 1), which is sufficiently stable to be observed in the $^{31}P\{^1H\}$ NMR spectrum, appearing as signals at ca. 10 ppm (for the σ^4P center) and ca. 266 ppm (for the σ^2P) correlated by the common $^2J_{PP}$ value. The ^{19}F NMR spectrum also shows signals due to the fluorine atoms on the exo-phosphorus center

Scheme 1. Formation of the Monomeric Compounds **7** and **8** and the Possible Route to the Dimeric (Difluorophosphorano)diazaphospholes (R = mes*, *p*-MePh)[a]

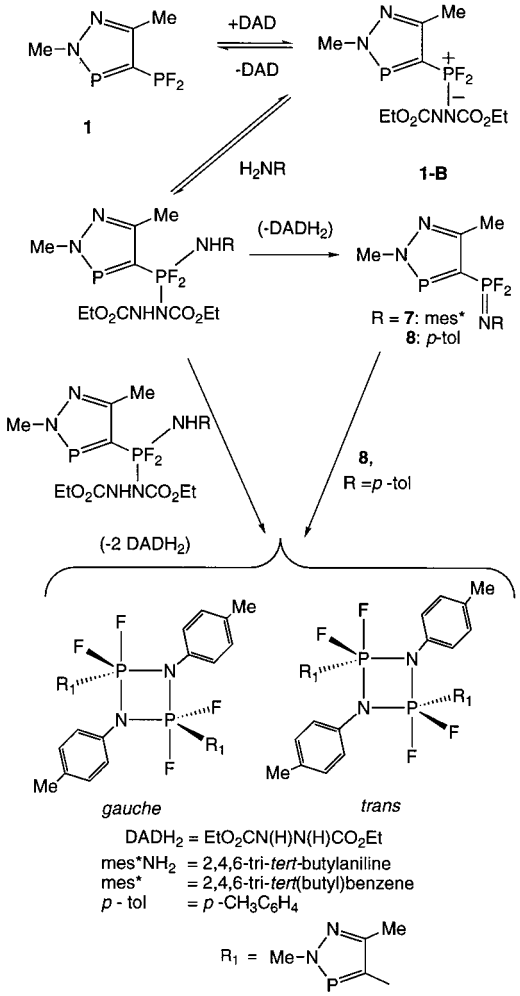

[a] The gauche and trans isomers of the dimer of **8** are also illustrated.

of the betaine intermediate (at −27.30 ppm), and these fluorine atoms are coupled to both phosphorus centers ($^1J_{\sigma^3PF}$ = 971 Hz, $^3J_{\sigma^2PF}$ = 51 Hz). The major final product, **7**, obtained from the bulky amine (mes*NH_2) showed a $^{31}P\{^1H\}$ NMR signal for the exo-phosphorus at −40.56 ppm and a signal for the endo-phosphorus at 266.38 ppm correlated with a common $^2J_{PP}$ value of 88 Hz. The ^{19}F NMR spectrum of **7** showed a doublet of doublets for the fluorines on the phosphorus center (−58.47 ppm, $^1J_{\sigma^3PF}$ 1079 Hz, $^3J_{\sigma^2PF}$ 10 Hz) which was shifted downfield relative to the parent compound **1**. Neither the betaine nor the (iminophosphorano)diazaphospholes (both **7** and **8**) could be isolated because the diethyl-1,2-hydrazinedicarboxylate ($DADH_2$) produced during this redox condensation reaction possesses physical properties similar to those of the iminophosphoranes. Methodology developed for related systems[17,20] failed to provide separations in the present system, and the route was not pursued.

The bulk of the amine controls the reaction. The smaller amine, *p*-toluidine, gave, as the major product, the dimerized four-membered-ring phosphetidine system, and we surmise that, in this case, the betaine intermediate must also be relatively stable. The more bulky amine, tri-2,4,6-*tert*-butylaniline, favored the formation of the monomeric iminophosphorane **7**, with only

(18) Gololobov, Y. G.; Zhmurova, I. N.; Kasukhin, L. F. *Tetrahedron* **1981**, *37*, 437−472.
(19) Gololobov, Y. G.; Kasukhin, L. F. *Tetrahedron* **1992**, *48*, 1353−1406.
(20) Bittner, S.; Pomerantz, M.; Assaf, Y.; Krief, P.; Xi, S.; Witczak, M. K. *J. Org. Chem.* **1988**, *53*, 1−5.

a small amount of the dimeric species being observed in the ^{19}F NMR spectrum.

Examination of NMR spectra of the *p*-toluidine system revealed also fluxional behavior and the presence of isomers. The phosphorus NMR signal for the σ^2P center consisted of one set of doublets (266.41 ppm, $^2J_{PP}$ 96 Hz). The region due to the exo-phosphorus revealed two sets of signals, one of which was sharp and corresponded to the iminophosphorane **8**; the remainder of the signal was broad with a second-order appearance. Similar phosphorus−fluorine coupling constants could be identified within these spectral patterns. The ^{19}F NMR spectrum of the reaction mixture revealed that three species were present, all of which carried a *p*-toluidine functionality on the nitrogen. The fluorine resonance of this iminophosphorane, **8**, was found at −58.52 ppm ($^1J_{\sigma^3PF}$ 1077 Hz, $^3J_{\sigma^2PF}$ 10 Hz). An additional aminophosphorane species showed chemical shifts for inequivalent fluorine environments with one fluorine resonance at −27.27 ppm ($^1J_{\sigma^5PF}$ 756 Hz, $^3J_{\sigma^2PF}$ 10 Hz, $^2J_{FF}$ 90.9 Hz, $^4J_{FF}$ 12.3 Hz) and the other fluorine resonance at −33.18 ppm, which was slightly broadened ($^1J_{\sigma^5PF}$ 734 Hz, $^2J_{FF}$ ∼80 Hz). A third species showed a broad signal at −49.15 ppm ($^1J_{\sigma^5PF}$ 896 Hz). When the NMR sample was cooled to −10 °C, two signals emerged from the broadened resonance at −51.33 ppm ($^1J_{\sigma^5PF}$ 871 Hz), and −47.38 ppm ($^1J_{\sigma^5PF}$ 910 Hz). These sets of signals may be reasonably assigned to gauche and trans isomers of the expected four-membered 1,3,2,4-diazaphosphetidine ring system (Scheme 1) of the dimer of **8**. Similar behavior has been described for related diazaphosphetidines, $[RF_2PNMe]_2$ (R = Me, Et, OMe).[21] It is not clear whether the betaine intermediate is essential for the formation of the dimer, as tentatively suggested in Scheme 1, or if the monomer is the first product formed in all cases and the species with the less bulky substituents then dimerize independently.

NMR Spectroscopic Characterization and Trends. The compounds are readily identified from the diagnostic ^{31}P and ^{19}F spectra. In addition, the ^{13}C and ^1H NMR spectral parameters are useful. Values are given in Tables 1−4 with some additional minor parameters given in the Experimental Section. The exocyclic center of all oxidized products **4**−**14** was characterized by upfield $^{31}P\{^1H\}$ NMR spectral shifts relative to those of the unoxidized phosphines,[10] which in some cases were quite large, whereas the endocyclic phosphorus center was essentially unchanged or displayed a small downfield shift. The phosphorus NMR signals were correlated by a common $^2J_{PP}$ coupling which varied upon oxidation. This coupling constant increased relative to that of the parent phosphine in the case of all chalcogeno derivatives and for the imido derivatives of **2** and **3**, two systems where the parent phosphines had very small $^2J_{PP}$ coupling constants. The $^2J_{PP}$ coupling constant however decreased upon formation of the imido derivatives of **1**. The derivatives of **1** also showed large diagnostic one-bond phosphorus−fluorine coupling constants for the derivatives **4**−**8**. There were some contrasting differences; for example, $^1J_{PF}$ for the thioxo derivative, **4**, was smaller than that for the parent phosphine, **1**,[10] whereas the coupling in the selenoxo analogue, **5**, was larger. In all cases, the endocyclic phosphorus center shifted by a small amount downfield upon oxidation of the other center.

These observed shift changes accompanying oxidation contrast with the general behavior of alkylated or arylated phosphines, for which the phosphorus chemical shift signal moves downfield upon oxidation. We previously observed however that monooxidation of bis(diphenylphosphino)methane (dppm) with trimethylsilyl azide induced a large downfield shift ($\Delta\delta$) of 21.1 ppm for the resonance of the oxidized phosphorus center with a concomitant small upfield shift (of 5.2 ppm) for the remaining P(III) center.[22] Such a downfield shift is expected as a result of the increased deshielding of the oxidized phosphorus center. Halogenated phosphines however show a behavior opposite to that of our compounds. For example, the chemical shifts of both OPF_3 (−36 ppm) and $OPCl_3$ (2 ppm) lie upfield from the shifts of the unoxidized PF_3 (97 ppm) and PCl_3 (219 ppm). The oxidized shift change upon oxidation of PF_3 to OPF_3 has been calculated[23] and is in good agreement with the experimental measurement.

The $^{13}C\{^1H\}$ NMR spectra are of interest and are useful for identification purposes because of the prominent P−C coupling constants displayed by these compounds.[10] The fluorinated sulfido and the selenido phosphoranodiazaphosphole compounds **4** and **5** also showed a two-bond fluorine−carbon coupling (E = S, 24 Hz; E = Se, 24 Hz) which was not observed for the parent compound **1**.[10] Oxidation of the exocyclic phosphorus also induced a large increase in the $^1J_{\sigma^2PC}$ endocyclic phosphorus couplings (to approximately 120−160 Hz), an interaction which is small (ca. 35 Hz) in the unoxidized phosphinodiazaphospholes **1**−**3**.[10] Associating the one-bond phosphorus−carbon coupling constant with the degree of "s" character in the P−C bond suggests that the oxidation process enhances the "s" character of the bond between the exo-phosphine and the ring carbon.

Upon oxidation, the $^2J_{PC}$ values involving both phosphorus centers and the carbon at the 5-position ($^2J_{\sigma^2PC} = {}^2J_{\sigma^4PC} = 5$ Hz) generally decreased. The 2-methyl carbon signal also tended to shift slightly upfield (ca. 40 ppm), and a moderate value of $^2J_{\sigma^2PC}$ was observed (∼0.20 Hz). The methyl group carbon atoms attached to the 5-position (ca. 16 ppm) did not in general show any coupling to phosphorus.

Coupling to ^{19}F also appeared strongly in the spectra of both the sulfido and the selenido phosphoranodiazaphospholes; the spectra of **4** and **5** showed a doublet of doublets pattern. Oxidation of the exo-phosphorus also had a deshielding effect on the fluorine signals, and there was a large decrease in the long-range coupling of the fluorine atoms to the σ^2P center relative to the parent phosphinodiazaphosphole, **1**. The fluorine NMR signal of **5** showed further coupling to the selenium (104 Hz), which was also reflected in the ^{77}Se NMR spectrum. The ^{19}F NMR spectra of the oxidized compounds **13** and **14** were greatly simplified, changing from the doublet of doublet of triplets observed for the parent phosphine **3** to a simple triplet. The chemical shift values were however essentially unchanged after oxidation of the exo-phosphorus center, and the resonances showed coupling to only the methylene protons. The chemical shifts of the ortho and the meta fluorine resonances for the tfbn ring were observed at −152.95 ppm ($^4J_{\sigma^4PF}$ 5.7 Hz) and 140.95 ppm, respectively. Similar patterns were observed for the other homologues.

The proton signals in the ^1H NMR spectra of both **4** and **5** were relatively unaffected by oxidation of the exo-phosphorus center. Only small downfield shifts were observed for the 2-methyl group proton signals of **4** and a small upfield shift was observed in the resonance for **5**. Both compounds showed an increase in the phosphorus−proton coupling constant (to ca. 8.6 Hz) upon oxidation. The 4-methyl group proton resonances shifted downfield in the case of **4**, and coupling was observed

(21) Harris, R. K.; Wazeer, M. I. M.; Schlak, O.; Schmutzler, R. *Phosphorus Sulfur* **1981**, *11*, 221−239.

(22) Katti, K. V.; Batchelor, R. J.; Einstein, F. W. B.; Cavell, R. G. *Inorg. Chem.* **1990**, *29*, 808−814.

(23) Bernard-Moulin, P.; Pouzard, G. *J. Chim. Phys.* **1979**, *76*, 708−713.

to the exo-phosphorus center (2.39 ppm, $^4J_{PH}$ 0.9 Hz), whereas the protons of the same group in **5** were unchanged (2.51 ppm). In neither case was coupling to either phosphorus center observed.

NMR Spectroscopic Characterization of 6. As was the case for the chalcogens, oxidation of the exo-phosphine center of **1** to form **6** resulted in a large upfield ^{31}P NMR shift of over 200 ppm relative to that of the parent phosphine with a concomitant downfield shift for the σ^2P signal to 265.70 ppm. In contrast to the case of the chalcogen derivatives of **2** and **3**, for which $^2J_{PP}$ increased on oxidation, the $^2J_{PP}$ value of all derivatives of **1** remained relatively unchanged or decreased slightly with the phosphine oxidation. Direct $^1J_{\sigma^4PF}$ coupling was slightly reduced (1145 Hz) as was the longer range $^3J_{\sigma^2PF}$ coupling (6 Hz), a trend which parallels the behavior of the chalcogen derivatives.

The ^{13}C{^{1}H} NMR spectrum of **6** shows a shift of 10 ppm downfield for the carbon at the 4-position upon oxidation. As was the case for **4** and **5**, there was an increase in the both phosphorus−carbon coupling constants ($^1J_{\sigma^2PC}$ 246 Hz, $^1J_{\sigma^4PC}$ 45 Hz) and a $^4J_{CF}$ coupling was observed (24 Hz) which was not observed in the spectrum of the parent fluorophosphine. The large increase in the phosphorus−carbon coupling constant may be explained in terms of the participation of resonance structures illustrated in Figure 2.

Infrared Spectroscopic Properties. Both oxidized difluorophosphino derivatives **4** and **5** showed characteristic P−F stretching frequencies which were higher than those of the parent phosphine **1** (E = S, ν(P−F) = 853, 823 cm^{-1}; E = Se, ν(P−F) = 869, 841 cm^{-1}), in keeping with the general trend of increased P−F stretching frequencies for pentavalent phosphorus−fluorine compounds compared to the trivalent precursors.[24,25] The thioxo derivatives showed a strong band attributable to ν(P═S) (**4**, 726 cm^{-1}; **9**, 723 cm^{-1}) and likewise the selenoxo compounds showed a band attributable to ν(P═Se) (**5**, 533 cm^{-1}; **10**, 542 cm^{-1}; **13**, 542 cm^{-1}). The imido derivatives also showed characteristic bands due to ν(P═N) (**11**, 1377 cm^{-1}; **6**, 1498 cm^{-1}; **12**, 1492 cm^{-1}; **14**, 1489 cm^{-1}). **11**, a silylated imine, possesses properties similar to those of other P═NSiMe$_3$ compounds that we have prepared,[9,22] and likewise **6**, **12**, and **14**[26,27] have properties similar to those of the tfbn imide. The tfbn substituent also shows characteristic ν(CN) frequencies (**6**, 2241 cm^{-1}; **12**, 2237 cm^{-1}; **14**, 2237 cm^{-1}), and these values are higher than those observed for the dppm analogues (2218−2233 cm^{-1}).[26,27] The P−F stretching frequencies were also shifted to higher frequencies upon oxidation of the exo-phosphorus atom (921 and 896 cm^{-1}) with the imide. A ν(P═N) vibration was observed at 1498 cm^{-1}.

Crystal and Molecular Structure of 6. The solid-state structure of **6** was determined. Crystal parameters and analysis details are given in Table 5, and selected metrical results are given in Tables 6 and 7. The molecular structure (Figure 1)[28] revealed two planar ring systems consisting of the diazaphosphole and the *p*-tetrafluorophenyl with an angle of 26.3° between the rings. The P(41)−N(41)−C(41) bond angle is 141.8(2)°, and the P(41)−N(41) and N(41)−C(41) bond lengths are 1.514(2) and 1.363(3) Å, respectively. The length of the phosphorus−nitrogen double bond is a little shorter than the range 1.54−1.64 Å predicted by the sum of Pauling double bond radii. The bond lengths and angles displayed by the phosphole ring system are similar to those of the diazaphosphole and are consistent with an aromatic system. The angle about the σ^2P center, N(2)−P(3)−C(4), is 88.25(11)°. This angle compares with that found for the parent diazaphosphole hydrochloride, Chart 2, **I** (88.2°),[29,30] and for the (aminochlorophosphino)-diazaphosphole, Chart 2, **II**,[31] showing that the diazaphosphole ring system is essentially unaffected by a change in the geometry at the exo-phosphorus. This is further supported by the relative constancy of the σ^2P NMR shift signal. The F(41)−P(41)−F(42) angle is 97.44(10)°, and the average of the P−F bond distances is 1.537 Å. This phosphorus−fluorine bond is longer than that observed for a related P(V) compound, Ph$_2$FP═NMe (1.488 Å),[32] which however must develop a more basic imine center as a result of the presence of a methyl as opposed to a tfbn substituent on the nitrogen.

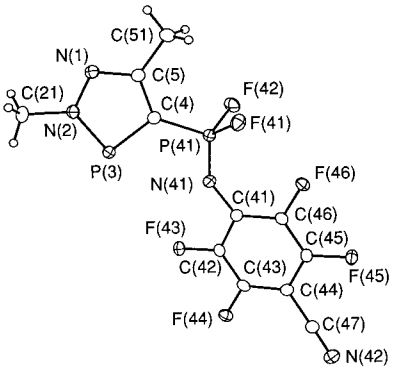

Figure 1. Perspective ORTEP[28] view of 4-(difluoro((*p*-cyanotetrafluorophenyl)imino)phosphorano)-2,5-dimethyl-2*H*-1,2,3σ^2-diazaphosphole (**6**) showing the atom-numbering scheme. Non-hydrogen atoms are represented by Gaussian ellipsoids at the 20% probability level.

Chart 2. Previously Structurally Characterized Diazaphospholes

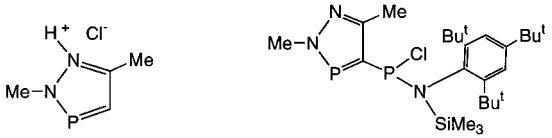

I **II**

The phosphorus−nitrogen double bond of **6** is short compared to those of other iminophosphines, as shown in Table 8. Such short P═N bond lengths are typically accompanied by an increase in the P═N−R angle. In the case of Ph$_2$FP═NMe, the P═N−C bond angle is 119° and the nitrogen can be considered to adopt classical sp^2-hybridized geometry. ((Trimethylsilyl)-imino)phosphoranes have, in general, very large P═N−Si bond angles (cf.: Ph$_2$PCH$_2$PPh$_2$(═NSiMe$_3$), ∠P═N−Si = 150°; Me$_3$P═NSiMe$_3$, ∠P═N−Si = 145°; 1-(Ph$_2$P)-2-(Ph$_2$P(═NSiMe$_3$))C$_6$H$_4$, ∠P═N−Si = 152°). In the case of **6**, the P═N−C bond angle (142°) is more open than those in most of the nonsilyl iminophosphoranes listed, and **6** also has one of the shortest P═N distances (1.514 Å). It is notable that two

(24) Daasch, L. W.; Smith, D. C. *Anal. Chem.* **1951**, *23*, 853.
(25) Thomas, L. C.; Chittenden, R. A. *Chem. Ind.* (*London*) **1964**, 1913.
(26) Imhoff, P.; Van Asselt, R.; Elsevier, C. J.; Vrieze, K.; Goubitz, K.; Van Malssen, K. F.; Stam, C. H. *Phosphorus, Sulfur Silicon* **1990**, *47*, 401−415.
(27) Mozol, V. J. M.Sc. Thesis, University of Alberta, 1993.
(28) Johnson, C. K. *ORTEP*; Report ORNL No. 5138; Oak Ridge National Laboratory: Oak Ridge, TN, 1976.
(29) Chernega, A. N.; Antipin, M. Y.; Struchkov, Y. T. *Russ. J. Struct. Chem.* (*Engl. Transl.*) **1988**, *29*, 265−303.
(30) Friedrich, P.; Huttner, G.; Luber, J.; Schmidpeter, A. *Chem. Ber.* **1978**, *111*, 1558−1563.
(31) Romanenko, W. D.; Rudzevich, V. L.; Gudima, A. O.; Sanchez, M.; Rozhenko, A. B.; Chernega, A. N.; Mazières, M. R. *Bull. Soc. Chim. Fr.* **1993**, *130*, 726−732.
(32) Adamson, G. W.; Bart, J. C. J. *J. Chem. Soc. A* **1970**, 1452−1456.

Table 5. Crystallographic Experimental Data for **6** and **15**

	6	**15**
	A. Crystal Data	
empirical formula	$C_{11}H_6F_6N_4P_2$	$C_{18}H_{33}Cl_2N_5P_2Ti$
fw	370.14	500.23
crystal dimensions (mm)	0.72 × 0.47 × 0.46	0.41 × 0.34 × 0.12
crystal system	triclinic	monoclinic
space group	$P\bar{1}$ (No. 2)	$P2_1$ (No. 4)
unit cell parameters	*a*	*b*
a (Å)	7.2744(15)	11.9477(11)
b (Å)	10.087(4)	8.4757(6)
c (Å)	10.566(2)	12.7567(11)
α (deg)	66.62(2)	
β (deg)	77.60(2)	108.824(8)
γ (deg)	78.14(3)	
V (Å^3)	688.8(4)	1222.7(2)
Z	2	2
ρ_{calcd} (g cm^{-3})	1.785	1.359
μ (cm^{-1})	3.88	6.321
	B. Data Collection and Refinement Conditions	
diffractometer	Enraf-Nonius CAD4[c]	Siemens P4/RA[d]
radiation (λ (Å))	Mo Kα (0.710 73)	Cu Kα (1.541 78)
temperature (°C)	−50	−60
crystal-to-detector distance (mm)	173	113.5
scan type	$\theta-2\theta$	$\theta-2\theta$
data collection 2θ limit (deg)	50.0	113.5
total no. of data collected	2554 ($-8 \le h \le 8, -10 \le k \le 11, 0 \le l \le 12$)	3646 ($-12 \le h \le 12, -9 \le k \le 9, -13 \le l \le 13$)[e]
no. of independent reflections	2411	3231
no. of observations	2030 ($F_o^2 \ge 2\sigma(F_o^2)$)	2891 ($F_o^2 \ge 2\sigma(F_o^2)$)
data/restraints/parameters	2411 [$F_o^2 \ge -3\sigma(F_o^2)$]/0/210	3218 [$F_o^2 \ge -3\sigma(F_o^2)$]/0/260
structure solution method	direct methods (SHELXS-86[f])	
refinement method	full-matrix least-squares on F^2 (SHELXL-93[g])	
absorption correction method	DIFABS[h]	semiempirical (Ψ scans)
range of transmission factors[h]	1.000−0.434	0.6907−0.2434
extinction coefficient		0.0037 (6)[i]
Flack absolute structure parameter[j]		−0.02 (2)
goodness-of-fit (*S*)[k]	1.067 [$F_o^2 \ge -3\sigma(F_o^2)$]	1.081 [$F_o^2 \ge -3\sigma(F_o^2)$]
final *R* indices[l]		
$F_o^2 > 2\sigma(F_o^2)$	$R_1 = 0.0368$, w$R_2 = 0.0968$	$R_1 = 0.0630$, w$R_2 = 0.1593$
all data	$R_1 = 0.0478$, w$R_2 = 0.1033$	$R_1 = 0.0768$, w$R_2 = 0.1973$
largest difference peak and hole (e Å^{-3})	0.442 and −0.348	0.406 and −0.429

[a] Obtained from least-squares refinement of 24 reflections with $18.0° < 2\theta < 29.7°$. [b] Obtained from least-squares refinement of 37 reflections with $54.1° < 2\theta < 57.9°$. [c] Programs for diffractometer operation and data collection were those supplied by Enraf-Nonius. [d] Programs for diffractometer operation and data collection were those of the XSCANS system supplied by Siemens. [e] Data were collected with indices of the form $+h,+k,\pm l$ and $-h,-k,\pm l$. [f] Sheldrick, G. M. *Acta Crystallogr.* **1990**, *A46*, 467−473. [g] Sheldrick, G. M. SHELXL-93: Program for crystal structure determination. University of Göttingen, Germany, 1993. Refinement on F_o^2 for all reflections (except in the case of **15**, where 13 having $F_o^2 < -3\sigma(F_o^2)$ were excluded). Weighted *R* factors wR_2 and all goodness-of-fit values (*S*) are based on F_o^2; conventional *R* factors R_1 are based on F_o, with F_o set to 0 for negative F_o^2. The observed criterion of $F_o^2 > 2\sigma(F_o^2)$ is used only for calculating R_1 and is not relevant to the choice of reflections for refinement. *R* factors based on F_o^2 are statistically about twice as large as those based on F_o, and *R* factors based on all data will be even larger. [h] Walker, N.; Stuart, D. *Acta Crystallogr.* **1983**, *A39*, 158−166. Transmission factors are equivalent transmission factors based on intensity. [i] $F_c^* = kF_c[1 + x\{0.001F_c^2\lambda^3/\sin(2\theta)\}]^{-1/4}$, where *k* is the overall scale factor. [j] Flack, H. D. *Acta Crystallogr.* **1983**, *A39*, 876−881. The Flack parameter will refine to a value near 0 if the structure is in the correct configuration and will refine to a value near 1 for the inverted configuration. [k] $S = [\sum w(F_o^2 - F_c^2)^2/(n-p)]^{1/2}$ (n = number of data; p = number of parameters varied; $w = [\sigma^2(F_o^2) + (aP)^2 + bP]^{-1}$ where $P = [\mathrm{Max}(F_o^2, 0) + 2F_c^2]/3$). For **6**, $a = 0.0600$ and $b = 0.3771$; for **15**, $a = 0.0936$ and $b = 4.3804$. [l] $R_1 = \sum||F_o| - |F_c||/\sum|F_o|$; w$R_2 = [\sum w(F_o^2 - F_c^2)^2/\sum w(F_o^4)]^{1/2}$.

Table 6. Selected Interatomic Distances (Å) for 4-(Difluoro((*p*-cyanotetrafluorophenyl)imino)phosphorano)-2,5-dimethyl-2*H*-1,2,3σ^2-diazaphosphole (**6**)

P(3)−N(2)	1.664(2)	N(2)−C(21)	1.457(3)
P(3)−C(4)	1.717(3)	N(41)−C(41)	1.363(3)
P(41)−F(41)	1.539(2)	N(42)−C(47)	1.136(3)
P(41)−F(42)	1.536(2)	C(4)−C(5)	1.417(3)
P(41)−N(41)	1.514(2)	C(5)−C(51)	1.489(4)
P(41)−C(4)	1.720(2)	C(41)−C(42)	1.403(3)
F(43)−C(42)	1.343(3)	C(41)−C(46)	1.392(3)
F(44)−C(43)	1.340(3)	C(42)−C(43)	1.370(4)
F(45)−C(45)	1.335(3)	C(43)−C(44)	1.382(3)
F(46)−C(46)	1.339(3)	C(44)−C(44)	1.391(3)
N(1)−N(2)	1.357(3)	C(44)−C(47)	1.433(3)
N(1)−C(5)	1.322(3)	C(45)−C(46)	1.374(3)

compounds with the same imino substituent, $NSiMe_3$, have different P═N bond lengths and P−N−Si angles; the P═N bond is shorter and the angle wider in the case of the diazaphosphole backbone as compared to the CH_2 backbone system of $Ph_2PCH_2PPh_2$(═Ntfbn),[33] suggesting that the diazaphosphole-phosphine backbone interacts with the phosphine imine substituent. The electron-withdrawing ability of the tfbn group in this system suggests that the resonance structure **C** in Figure 2 may play a dominant role in the description of the structure of the compound. As mentioned earlier, the P−F bond distance of 1.537 Å in **6**, although longer than the distance in Ph_2FP═NMe, is shorter than that usually observed (1.58 Å),[34] which may also be a result of the increase in induced positive charge

(33) Katti, K. V.; Santarsiero, B. D.; Pinkerton, A. A.; Cavell, R. G. *Inorg. Chem.* **1993**, *32*, 5919−5925.
(34) Corbridge, D. E. C. *The Structural Chemistry of Phosphorus*; Elsevier Scientific Publishing Co.: New York, 1974; p 7.

Table 7. Selected Interatomic Angles (deg) for 4-(Difluoro((*p*-cyanotetrafluorophenyl)imino)phosphorano)-2,5-dimethyl-2*H*-1,2,3σ^2-diazaphosphole (**6**)

N(2)−P(3)−C(4)	88.25(11)	N(41)−C(41)−C(46)	125.4(2)
F(41)−P(41)−F(42)	97.44(10)	C(42)−C(41)−C(46)	116.0(2)
F(41)−P(41)−N(41)	117.85(11)	F(43)−C(42)−C(41)	119.3(2)
F(41)−P(41)−C(4)	106.65(11)	F(43)−C(42)−C(43)	118.9(2)
F(42)−P(41)−N(41)	114.81(11)	C(41)−C(42)−C(43)	121.8(2)
F(42)−P(41)−C(4)	108.60(11)	F(44)−C(43)−C(42)	119.0(2)
N(41)−P(41)−C(4)	110.46(12)	F(44)−C(43)−C(44)	119.5(2)
N(2)−N(1)−C(5)	109.4(2)	C(42)−C(43)−C(44)	121.5(2)
P(3)−N(2)−N(1)	117.7(2)	C(43)−C(44)−C(45)	117.4(2)
P(3)−N(2)−C(21)	125.7(2)	C(43)−C(44)−C(47)	121.5(2)
N(1)−N(2)−C(21)	116.6(2)	C(45)−C(44)−C(47)	121.1(2)
P(41)−N(41)−C(41)	141.8(2)	F(45)−C(45)−C(44)	119.5(2)
P(3)−C(4)−P(41)	121.13(14)	F(45)−C(45)−C(46)	119.4(2)
P(3)−C(4)−C(5)	110.5(2)	C(44)−C(45)−C(46)	121.1(2)
P(41)−C(4)−C(5)	128.3(2)	F(46)−C(46)−C(41)	119.0(2)
N(1)−C(5)−C(4)	114.2(2)	F(46)−C(46)−C(45)	118.8(2)
N(1)−C(5)−C(51)	118.7(2)	C(41)−C(46)−C(45)	118.8(2)
C(4)−C(5)−C(51)	127.1(2)	N(42)−C(47)−C(44)	179.4(3)
N(41)−C(41)−C(42)	118.7(2)		

Table 8. Structural Data for N-Substituted Iminophosphoranes

compd	P═N (Å)	P═N−R (deg)	ref
6	1.514	141.8	this work
$Ph_2PCH_2PPh_2$(═NR)			
R = 5-F-2,4-$(NO_2)_2C_6H_2$	1.589	128.8	33
R = 4-$(CN)C_6F_4$	1.567	132.9	33
R = $SiMe_3$	1.529	150.2	42
Ph_3P═NPh	1.602	130.4	43
Ph_3P═NC_6H_4-*p*-Br	1.567	124.2	44
Ph_3P═NCN	1.595	123.0	45
Ph_3P═$NP(CF_3)_2$	1.576	131.0	46
1-(Ph_2P)-2-(Ph_2P(═$NSiMe_3$))C_6H_4	1.529	152.7	9
Me_3P═$NSiMe_3$[a]	1.542	144.6	47
Ph_2FP═NMe	1.641	119.1	32
15	1.592	161.3	this work

[a] Gas-phase electron diffraction structure.

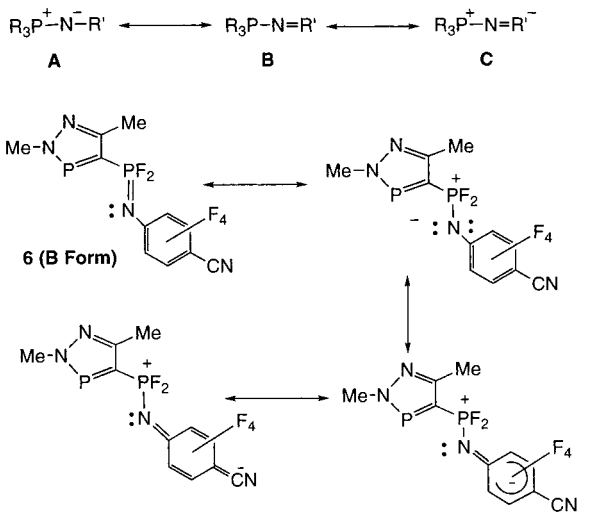

Figure 2. Resonance forms of the general λ^5-iminophosphorane system and for the specific case of compound **6**.

on the phosphorus(V) atom arising from resonance delocalization into the tfbn moiety.

The electronic structures of λ^5-iminophosphoranes are similar to those of the phosphine oxides and ylides and can be represented as either the dipolar resonance form, **A**, or the multiple P═N bond (Figure 2).[35,36] In the **B** form, pπ−dπ multiple bonding (or p−σ* overlap) may be proposed.[35] An additional form, **C**, can also be written if the group R′ can further participate in resonance structures. The iminophosphoranes differ from the phosphonium ylides in that they are less stable because the suitable vacant orbitals on the carbon atom are of lower energy than those offered by nitrogen. These resonance forms then suggest that the phosphorus(V) center would become more positive by means of the dipole changes induced by delocalization into the *p*-cyanotetrafluorophenyl group. This property would then shorten the phosphorus−carbon bond, and the resultant increase of the P−C "s" character would be reflected in an increase in $^1J_{PC}$. There was also a marked increase in $^2J_{\sigma^2PC}$ (45 Hz) for the methyl carbon at the 4-position (125.17 ppm). The carbon at the 5-position was coupled only to the exo-phosphorus (158.21 ppm, $^2J_{\sigma^4PC}$ 13 Hz), while the resonance for the methyl group appeared as a singlet (15.01 ppm).

The ^{19}F NMR spectrum demonstrated, through the chemical shift of the fluorine atoms on the exo-phosphorus center, that these atoms were not as deshielded as was the case with the chalcogen derivatives (−56.54 ppm). The observed value of $^3J_{\sigma^2PF}$ (34 Hz) was similar to that displayed by **4**. The chemical shifts for the ortho and the meta fluorines on the tfbn ring were −152.81 ppm ($^4J_{\sigma^4PF}$ 5.7 Hz) and 139.77 ppm, respectively. The ^{1}H NMR signals of the methyl group at the 2-position (4.14 ppm, $^3J_{\sigma^2PC}$ 8.9 Hz) and the methyl group at the 4-position (2.61 ppm) of the ring were essentially unchanged by imine formation.

Attempted Oxidation of the Dicoordinate Phosphorus Center in 4-(Bis((dimethylamino)thioxophosphorano))-2,5-dimethyl-2*H*-1,2,3σ^2-diazaphosphole (9). In view of the great stability of the oxidized exo-phosphorus center in 4-(bis-((dimethylamino)thioxophosphorano))-2,5-dimethyl-2*H*-1,2,3σ^2-diazaphosphole (**9**), we wondered if it would be possible to also oxidize the endocyclic dicoordinate phosphorus(III) center in this system. Therefore, **9** was treated with an excess of trimethylsilyl azide in refluxing toluene for a period of 24 h. Removal of the volatile materials in vacuo indicated, according to the ^{31}P{^{1}H} NMR spectrum of the remaining material, that no oxidation (or transformation) had occurred. Therefore, in all cases for this system, the oxidation of the substituted phosphinodiazaphospholes with either chalcogens or azides occurred only at the exo-phosphorus center to give the σ^2P−σ^4P phosphine−phosphorane system. We conclude that the two-coordinate phosphorus center does not act as a typical phosphine because the lone pair is not in an appropriate orbital to allow the oxidation reaction of either type to proceed. This implies that the orbitals of the two-coordinate P(III) center are delocalized into the ring and thus this center is neither basic nor oxidizable in the usual sense of phosphorus(III) behavior. The σ^2 phosphorus center is however known to form metal complexes, but the factors which enhance or inhibit this behavior are not yet clear.[37−39] Steric interactions with reagents are unlikely because the diazaphosphole has a planar ring system, which does not provide extensive bulk, as will be demonstrated in following papers.

Trans metalation of 11: Synthesis of [(η^5-C_5Me_5)$TiCl_2$-(N═P(NMe_2)$_2$(2,5-dimethyl-2*H*-1,2,3σ^2-diazaphosphol-

(35) Gilheany, D. G. *Chem. Rev.* **1994**, *94*, 1339−1374.
(36) Johnson, A. W. *Ylides and Imides of Phosphorus*; Wiley: New York, 1993.
(37) Kraaijkamp, J. G.; van Koten, G.; Vrieze, K.; Grove, D. M.; Klop, E. A.; Spek, A. L.; Schmidpeter, A. *J. Organomet. Chem.* **1983**, *256*, 375−389.
(38) Kraaijkamp, J. G.; Grove, D. M.; van Koten, G.; Schmidpeter, A. *Inorg. Chem.* **1988**, *27*, 2612−2617.
(39) Weinmaier, J. H.; Tautz, A.; Schmidpeter, A.; Pohl, S. *J. Organomet. Chem.* **1980**, *185*, 53−68.

Table 9. Selected Interatomic Distances (Å) for [(η^5-C_5Me_5)$TiCl_2$(N═P(NMe_2)$_2$(2,5-dimethyl-2*H*-1,2,3σ^2-diazaphosphol-4-yl))] (**15**)

Ti−Cl(1)	2.306(3)	N(11)−C(11)	1.472(11)
Ti−Cl(2)	2.314(3)	N(11)−C(12)	1.457(13)
Ti−N(1)	1.781(6)	N(12)−C(13)	1.473(12)
Ti−C(20)	2.368(8)	N(12)−C(14)	1.450(11)
Ti−C(21)	2.436(7)	C(4)−C(5)	1.411(10)
Ti−C(22)	2.448(8)	C(4)−C(7)	1.507(12)
Ti−C(23)	2.382(9)	C(20)−C(21)	1.446(11)
Ti−C(24)	2.347(9)	C(20)−C(24)	1.432(11)
P(1)−N(2)	1.669(6)	C(20)−C(25)	1.488(12)
P(1)−C(5)	1.721(7)	C(21)−C(22)	1.400(11)
P(2)−N(1)	1.592(6)	C(21)−C(26)	1.487(11)
P(2)−N(11)	1.651(7)	C(22)−C(23)	1.428(12)
P(2)−N(12)	1.645(7)	C(22)−C(27)	1.479(12)
P(2)−C(5)	1.778(7)	C(23)−C(24)	1.387(12)
N(2)−N(3)	1.363(9)	C(23)−C(28)	1.498(13)
N(3)−C(4)	1.330(10)	C(24)−C(29)	1.506(12)
N(2)−C(6)	1.464(9)		

4-yl))] (15). (((Trimethylsilyl)imino)phosphorano)diazaphosphole **11** reacted readily with Cp^*TiCl_3 at elevated temperatures in acetonitrile, smoothly replacing the silyl group with the titanium moiety to form **15** (eq 6). Full spectral parameters are given in

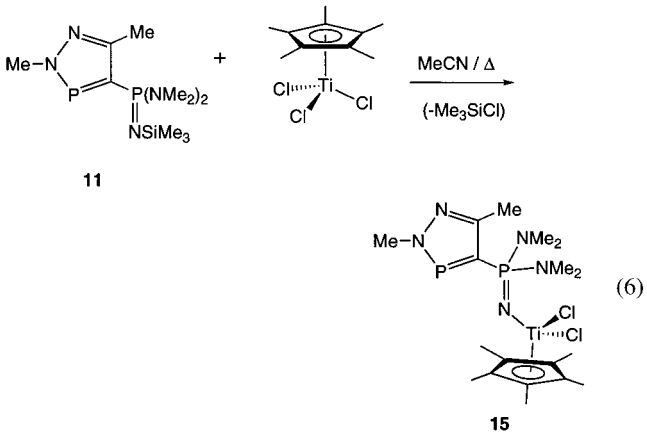

(6)

the Experimental Section.

The $^{31}P\{^1H\}$ NMR spectrum shows a shift to a lower field for the two-coordinate phosphorus center (260.87 ppm) resonance and a shift of 34 ppm to 40.87 ppm downfield for the iminophosphorane center signal. The $^2J_{PP}$ value increases to 84 Hz. The carbon signal for the methyl groups of the trimethylsilyl moiety (3.56 ppm for **9**) disappears from the $^{13}C\{^1H\}$ NMR spectrum with the loss of trimethylsilyl chloride, thus providing evidence for the formation of the titanium−nitrogen σ bond. The infrared spectrum shows a strong absorption at 1091 cm^{-1} due to the antisymmetric stretch vibration of the P−N−Ti group. For a comparison, related Ti−N−P linkages show asymmetric stretching frequencies ranging from 986 cm^{-1} for $CpTiCl_2(NPMe_3)$[40] to 1110 cm^{-1} for $[Ph_2P(NSiMe_3)_2]Ti(NPNSiMe_3)$.[41]

The solid-state structure of **15** was determined. Crystal details and procedures are given in Table 5, and selected metrical results are given in Tables 9 and 10. The structure, illustrated in Figure 3,[28] shows a N(2)−P(1)−C(5) angle within the diazaphosphole ring of 89.3(3)°, which is similar to those shown by other diazaphospholes, including **6**, whose structure is described above. One notable feature of the structure is the very large

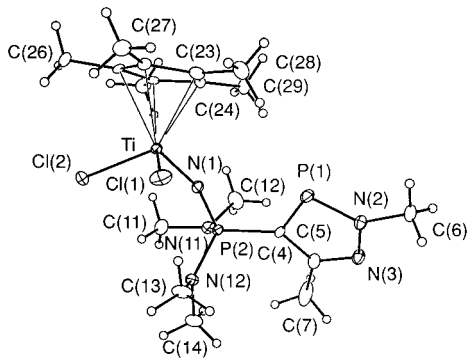

Figure 3. Perspective ORTEP[28] view of [(η^5-C_5Me_5)$TiCl_2$(N═P(NMe_2)$_2$-(2,5-dimethyl-2*H*-1,2,3σ^2-diazaphosphol-4-yl))] (**15**) showing the core atom labeling scheme. Non-hydrogen atoms are represented by Gaussian ellipsoids at the 20% probability level,

Table 10. Selected Interatomic Angles (deg) for [(η^5-C_5Me_5)$TiCl_2$(N═P(NMe_2)$_2$(2,5-dimethyl-2*H*-1,2,3σ^2-diazaphosphol-4-yl))] (**15**)

Cl(1)−Ti−Cl(2)	102.71(12)	C(5)−P(2)−N(11)	108.4(4)
N(2)−N(3)−C(4)	108.5(6)	N(3)−C(4)−C(5)	116.1(7)
Cl(1)−Ti−N(1)	103.7(3)	C(5)−P(2)−N(12)	112.2(4)
P(2)−N(11)−C(11)	116.5(6)	N(3)−C(4)−C(7)	117.4(7)
Cl(2)−Ti−N(1)	101.7(2)	N(11)−P(2)−N(12)	102.0(4)
P(2)−N(11)−C(12)	119.4(7)	C(5)−C(4)−C(7)	126.4(7)
N(2)−P(1)−C(5)	89.3(3)	Ti−N(1)−P(2)	161.3(5)
C(11)−N(11)−C(12)	112.9(8)	P(1)−C(5)−P(2)	118.4(4)
N(1)−P(2)−C(5)	107.1(3)	P(1)−N(2)−N(3)	117.1(5)
P(2)−N(12)−C(13)	118.1(6)	P(1)−C(5)−C(4)	108.9(5)
N(1)−P(2)−N(11)	116.6(4)	P(1)−N(2)−C(6)	127.2(6)
P(2)−N(12)−C(14)	124.5(7)	P(2)−C(5)−C(4)	132.1(6)
N(1)−P(2)−N(12)	110.6(4)	N(3)−N(2)−C(6)	115.7(6)
C(13)−N(12)−C(14)	112.7(8)		

Ti−N−P angle of 161.3(5)°, much larger than similar angles for phosphine imines listed in Table 8.[42−47] Also the P═N distance is slightly shorter than those in the phosphine imines. If the bonding description of phosphine iminate complexes favors **C** with an end-on arrangement as shown in Figure 2, an M−N−P angle of 180° is to be expected. The Ti structures do not in general achieve this linearized P−N−M structure, perhaps because significant steric effects about the titanium metal center which arise in this case from the pentamethylcyclopentadienyl ring, the two dimethylamino groups, and the pendant phospole ring on the exo-phosphorus center inhibit such linearization. The Ti−N distance is however shorter than the sum of the single-bond covalent radii, suggesting enhanced binding of the phosphine iminate. The shortening of this bond may be a consequence of additional conjugation through the diazaphosphole ring which also appears to cause an increase in the $^2J_{PP}$ value. The P−N single bonds between the exo-phosphorus atom and the attached dimethylamino groups are also short (average 1.649 Å), suggesting that multiple-bond character extends to these nitrogen atoms as well.

Summary

The oxidation of phosphinodiazaphospholes which contain fluorines, amino groups, or alkoxy groups on the exo-phosphorus

(40) Rübenstahl, T.; Weller, F.; Harms, K.; Dehnicke, K.; Fenske, D.; Baum, G. *Z. Anorg. Allg. Chem.* **1994**, *620*, 1741−1749.
(41) Witt, M.; Roesky, H. W.; Stalke, D.; Pauer, F.; Henkel, T.; Sheldrick, G. M. *J. Chem. Soc., Dalton Trans.* **1989**, 2173−2177.
(42) Schmidbaur, H.; Bowmaker, G. A.; Kumberger, O.; Müller, G.; Wolfsberger, W. *Z. Naturforsch.* **1990**, *45B*, 476−482.
(43) Böhm, E.; Dehnicke, K.; Beck, J.; Hiller, W.; Strähle, J.; Maurer, A.; Fenske, D. *Z. Naturforsch.* **1988**, *43B*, 138−144.
(44) Hewlins, M. J. E. *J. Chem. Soc. B* **1971**, 942−945.
(45) Kaiser, J.; Hartung, H.; Richter, R. *Z. Anorg. Allg. Chem.* **1980**, *469*, 188−196.
(46) Ang, H. G.; Cai, Y. M.; Koh, L. L.; Kwik, W. L. *J. Chem. Soc., Chem. Commun.* **1991**, 850−852.
(47) Astrup, E. E.; Bouzga, A. M.; Ostoja Starzewski, K. A. *J. Mol. Struct.* **1979**, *51*, 51−59.

atom can be achieved with either chalcogens or azides. In all cases, exclusive oxidation occurred at the exo-phosphorus center. In general, the oxidation of the exo-phosphorus center resulted in a dramatic upfield shift of the phosphorus NMR signals attributable to this center and there was also a substantial increase in the $^1J_{PC}$ coupling constants, especially in the system with the *p*-cyanotetrafluorophenyl (tfbn) moiety on the imino group. Oxidation of the (difluorophosphino)diazaphosphole with diethyl azodicarboxylate gave the iminophosphorane with a 2,4,6-tri-*tert*-butylaniline (mes*) substituent, but with the smaller substituent on the imine nitrogen (*p*-toluidine), the iminophosphorane appears to dimerize readily to the cyclic diazadiphosphetidine, which was the major (but not the exclusive) product. Transmetalation yielded a titanium iminophosphorane which contained relatively short bonds and an open Ti−N═P angle, suggesting some delocalization in the core.

Acknowledgment. We thank the Natural Sciences and Engineering Research Council of Canada and the University of Alberta for financial support.

Supporting Information Available: Tables of crystallographic experimental details, non-hydrogen atom coordinates, bond lengths and angles, torsional angles, least-squares planes, anisotropic thermal parameters, and hydrogen atom coordinates for **6** and **15**. This material is available free of charge via the Internet at http://pubs.acs.org.

IC9802101